J Comput Aided Mol Des (2011) 25:145–161
DOI 10.1007/s10822-010-9406-9

DFT calculation of four new potential agents muscarinic of bispyridinium type: structure, synthesis, biological activity, hydration, and relations with the potents W84 and DUO-3O

M. Alcolea Palafox · P. Posada-Moreno · A. L. Villarino-Marín · C. Martinez-Rincon · I. Ortuño-Soriano · I. Zaragoza-García

Received: 10 September 2010 / Accepted: 5 December 2010 / Published online: 22 December 2010

Abstract Four new potential agents muscarinic (allosteric modulators) were synthesized and studied by using the B3LYP density functional method. The optimum conformation and geometry structure of these compounds were determined and analyzed. Solvent effects were considered including a variable number (1–15) of explicit water molecules surrounding the compound in order to simulate the first hydration shell, as well as using the Tomasi's polarized continuum model (PCM). A similar simultaneous analysis of the potents W84 and DUO-3O allosteric modulator of muscarinic receptors was also carried out. The effect of the hydration on the total atomic charges and several intermolecular distances of interest were also discussed. The biological activity against acetylcholine of our four synthesized bispyridinium salts was determined. Relationships/tendencies structure–activity were established. Several general conclusions were underlined.

Keywords Bispyridinium salts · W84 · DUO-3O · Geometry optimization · Hydration · DFT

M. Alcolea Palafox (✉)
Departamento de Química-Física I, Facultad de Ciencias Químicas, Universidad Complutense, 28040 Madrid, Spain
e-mail: alcolea@quim.ucm.es

P. Posada-Moreno · A. L. Villarino-Marín · C. Martinez-Rincon · I. Ortuño-Soriano · I. Zaragoza-García
Departamento de Enfermería, Escuela de Enfermería, Universidad Complutense, 28040 Madrid, Spain
e-mail: gerepa@enf.ucm.es

Introduction

Allosteric modulators (AM's) are agents that bind to a receptor and they can modify the efficacy or affinity of the endogenous ligand for its receptor. The FDA (U.S. Food and Drug Administration) has recently approved the first allosteric ligand (an allosteric enhancer acting on the calcium-sensing receptor) for the treatment of certain forms of secondary hyperparathyroidism and hypercalcemia [1, 2]. When the receptor is the muscarinic acetylcholine M_2 (subtype of muscarinic receptor highly sensitive to allosteric modulation), the effects could be beneficial in various disease states, for example, Alzheimer's disease (muscarinic M_2 receptors decrease in numbers with the progression of Alzheimer's syndrome [3]) or organophosphate poisoning.[1] Alzheimer's disease, the most common cause of senile dementia, is a complex neurological affection that affects to more than 20 million people worldwide [7]. On the other hand, pesticide exposure is recognized as an important environmental risk factor associated with cancer development [8].

Muscarinic receptors are glycoproteins located on the outer surface of the cell membrane, which contains two topographically-distinct ligand binding sites (Scheme 1): (1) the orthosteric site (or neurotransmitter binding site) for acetylcholine (ACh) and other conventional ligands, and (2) an allosteric site located at the entrance of the ligand binding cavity of the M_2 receptor [5, 9–12]. This allosteric site probably represents a subdomain of the receptor's allosteric binding cleft [13]. The M_2 receptor probably

[1] In the therapy of the poisoning by organophosphorus compounds, such as insecticides and nerve agents, e.g., sarin, the competitive antagonist atropine has been applied [4]; it can take advantage on the allosteric modulation [5, 6].

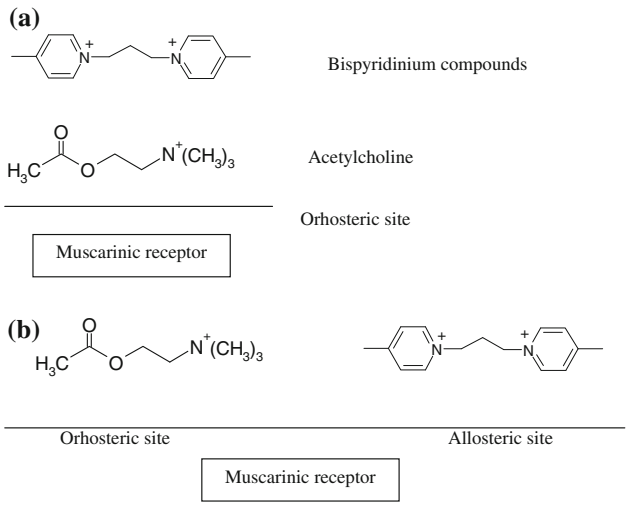

Scheme 1 Two possible mechanisms of action, in the orhosteric site and in the allosteric

contains more than one allosteric recognition sites on its extracellular face, because of bisquaternary compounds are very unlikely to pass cell membranes [14, 15].

As a consequence of the binding of the alloster to the receptor, the interaction between the ligand and the orthosteric binding site is altered [16].[2] The orthosteric and allosteric ligand may in a mutual fashion (enhance each other's binding), decrease it, or leave it unaffected, that is, cooperativity is positive, negative or neutral [17–19]. Appropriate AM's can elevate the binding and the action of ACh in a subtype-selective fashion [20, 21]. In view of the cooperative nature of interactions between allosteric and orthosteric ligands, it is likely that AM binding would also affect the conformation of the orthosteric site [22].

AM's have been extensively studied for biological properties, but few structural and energetic information obtained from theoretical calculations is available, and studies have not been reported using DFT methods. The starting point of the present study was the observation that several bispyridinium (bisbenzyl bispyridinium derivatives, so-called DUO series) compounds have shown to be potent AM's of muscarinic M_2 receptor [23–26]. Thus, the exploration of the conformational behavior of the bispyridinium compounds (4-acylaminomethylpyridinium dimers) is of great interest. For this purpose, four compounds were prepared in the present work for the first time, Scheme 2a: two new urea **Ia-b** derivatives and two ethylcarbamates **IIa-b** [27]. The present study of these compounds undertakes: (1) their conformational and structural study. For this task, DFT methods appear more accurate than MM simulations reported on AM's. (2) An initial study of their biological activity, comparing with the results obtained on ACh. (3) Their possible similarities comparing with the results obtained on the highly flexible W84 (one of the potent hexa-methonium-type modulators) and on DUO-3O, DUO-3C, Scheme 2b. Thus, the interest to obtain accurate results in the present manuscript. (4) The solvent effects on several parameters, simulating the first hydration shell. Since AM's have several specific sites for forming inter- and intramolecular hydrogen bonds, their conformers are strongly dependent on the solvent characteristics. (5) Finally, the structural parameters calculation in simpler compounds (Scheme 3), and their relations to the biological activity determined [28]. As consequence, several relationships and conclusions were underlined.

[2] Binding of allosteric ligands can induce conformational changes of the receptor that result in changes in receptor affinity for orthosteric agonists and antagonists.

Materials and methods

Synthesis

The synthesis of dimers **I** were performed following the literature procedure: [27] by reaction of 4-ureilmethylpyridinium salts **V** with piperidine as base in the presence of an oxidant agent as nitrobenzene (Scheme 4).

Melting points were determined on a Büchi 510 capillary melting point apparatus and they were uncorrected. Infrared (IR) spectra were recorded on a Perkin-Elmer 297. ^{1}H NMR spectra were recorded on a Varian T-60 (60 MHz) and T-90 (90 MHz) spectrometer for solutions in deuterated dimethylsulfoxide (DMSO-d_6). Splitting patterns were designated as s, singlet; d, double; t, triplet; q, quartet; m, multiplet. For multiplets either the center or the range of the multiplet were reported. Chemical shifts (δ) were calculated in ppm relative to tetramethylsilane as internal standard; coupling constants, J, were expressed in Hertz. Microanalyses were performed by Centro Nacional de Química Orgánica (CSIC). Reaction progress was monitored by TLC, using silica gel plates (Merck 60 F_{254}) and ethyl acetate as dissolvent.

N,N′-diaminocarbonyl-1,2-di(1-alkyl-4-pyridinium)ethylenediamine dihalides **I**: a solution containing 3,4 mmol of pyridinium salt, 15 mL of absolute ethanol, 4 drops of piperidine, and 4 drops of nitrobenzene, was heated to reflux for 4 h. After cooling, the solid was filtered and purified by recrystallization.

N,N′-diaminocarbonyl-1,2-di-(1-methyl-4-pyridinium)ethylenediamine diiodure **Ia**: Yield 85%; mp 240–242 °C (methanol); IR (KBr) 3,420 (NH), 3,320, 3,200 (NH_2), 1,670 (C=O), 1,640 (C=N), 1,570, 1,520 (Ar) cm^{-1}; ^{1}H NMR (DMSO-d_6) δ 4.6 (s, 6H, $2CH_3$), 5.4–5.6 (m, 2H, 2CH), 5.8 (s, 4H, $2NH_2$), 6.9–7.2 (m, 2H, 2NH), 8.2 (d, 4H, J = 6.0, pyridyl 2H-3, 2H-5), 9.1 (d, 4H, J = 6.0, pyridyl 2H-2, 2H-6) ppm. Anal. Calcd. for $C_{16}H_{22}I_2N_6O_2$: C,

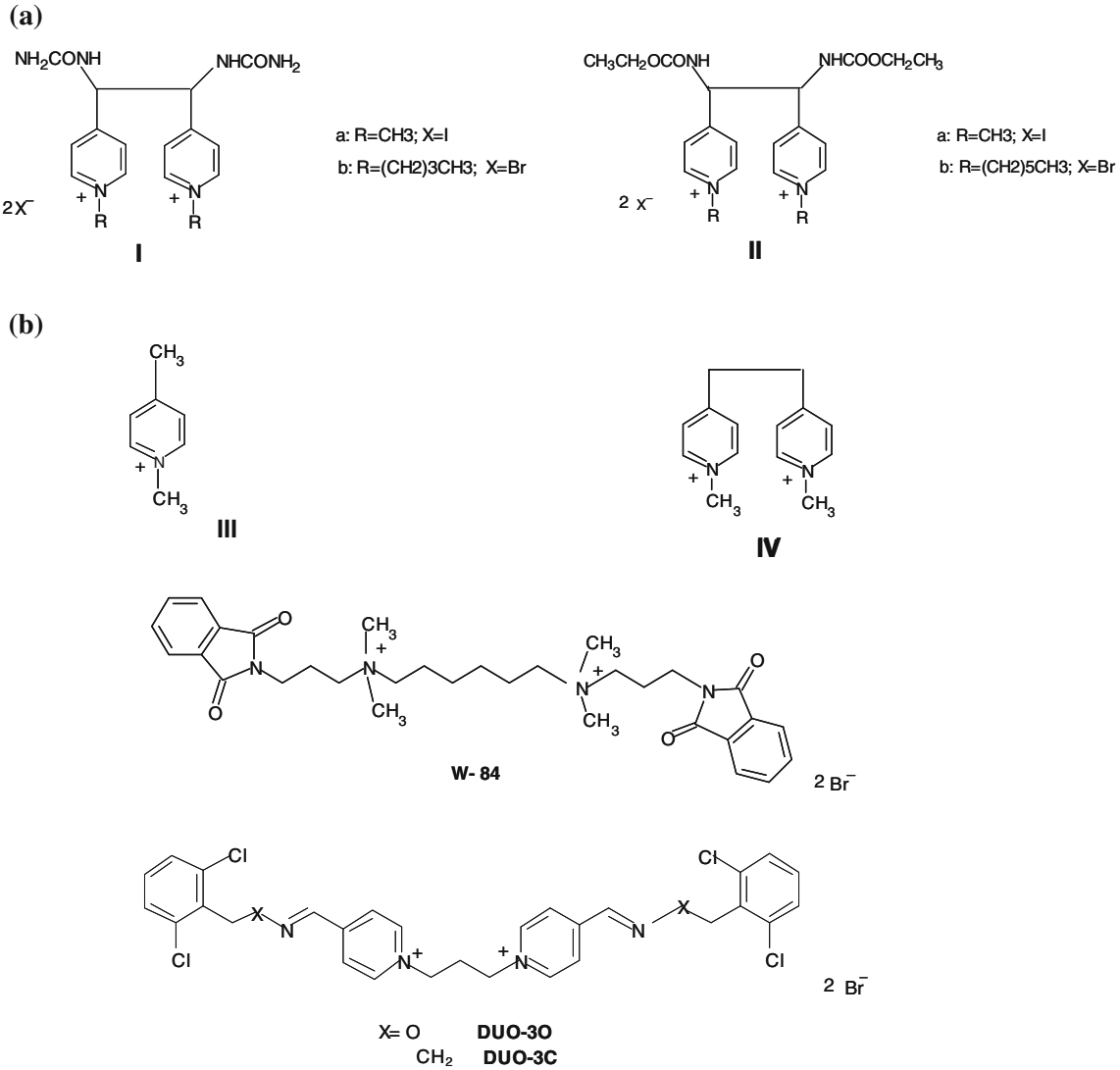

Scheme 2 (**a**) The four bispyridinium compounds studied Ia, Ib, IIa, and IIb; (**b**) other compounds included in the conformational and structural study

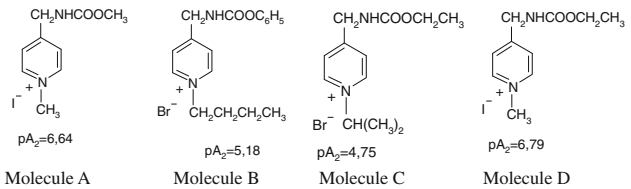

Scheme 3 Optimized molecules with the experimental value determined of pA_2

32.91; H, 3.77; N, 14.39; I, 43.47. Found C, 32.28; H, 3.98; N, 14.09; I, 43.55.

N,N′-diaminocarbonyl-1,2-di-(1-butyl-4-pyridinium)ethylenediamine dibromide **Ib**: Yield 50%; mp 257–259 °C (methanol); IR (KBr) 3,460 (NH), 3,320, 3,200 (NH_2), 1,680 (C=O), 1,640 (C=N), 1,610, 1,560 (Ar) cm^{-1}; ^1H NMR (DMSO-d_6) δ 0.9 (t, 6H, J = 7.5, $2CH_3$), 1.1–1.5 (m, 4H, $2CH_2$–C–C–N^+), 1.8–2.1 (m, 4H, $2CH_2$–C–N^+), 4.6 (t, 4H, J = 7.5, $2CH_2$–N^+), 5.2–5.4 (m, 2H, 2CH), 5.7 (s, 4H, $2NH_2$), 7.3–7.5 (m, 2H, 2NH), 8.2 (d, 4H, J = 5.9, pyridyl 2H-3, 2H-5), 9.2 (d, 4H, J = 5.9, pyridyl 2H-2, 2H-6) ppm. Anal. Calcd. for $C_{22}H_{34}Br_2N_6O_2$: C, 46.01; H, 5.92; N, 14.64; Br, 27.85. Found C, 46.14; H, 5.91; N, 14.42; Br, 27.62.

Biological assay: organ bath experiments

Isolated organ technique was carried out (muscle strips of the rat gastric fundus were mounted in organ bath for tension recordings) [29]. Female Whistar rats weighing 150–250 g were used in this study. The biological response depends on the dose of agonist in the isolated tissue preparation. In this case, the response was graded between zero and a maximal value. Biological results were average values obtained in triplicate.

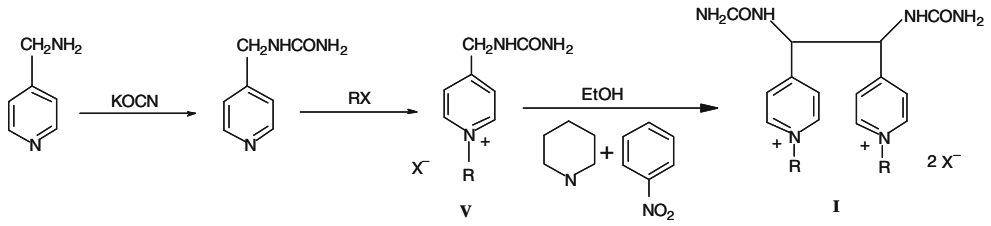

Scheme 4 General procedure of synthesis of acylaminomethylpyridinium dimers

The concentration proportion was as follows: control (acetylcholine) 1 μg/mL and compound (bispyridinium salt) 5 μg/mL. Concentration–response curves plot the percentage of maximal response (%E_{max}) versus the logarithm of the agonist concentration. The 50% effective dose (ED_{50}, the dose yielding half the maximum effect), the pA_2 (competitive antagonist) [30] or pD_2 (agonist), were obtained.

Computational methods

The molecules of Scheme 2 were studied by using Density Functional methods (DFT) [31], with the Becke's three-parameter exchange functional (B3) [32, 33] in combination with the correlational functional of Lee, Yang and Parr (LYP) [34]. DFT methods provide adequate compromise between the desired chemical accuracy and the heavy demands put on computer time and power. Moreover, they have been used satisfactory in many studies of drug design [35–37]. The B3LYP functional was chosen because different studies have shown that the data obtained with this level of theory are in good agreement with those obtained by other more computational costly methods, and it predicts vibrational wavenumbers better than the HF and MP2 methods [38–43].

Several basis set were used starting from 6-31G** to 6-311++G(3df,pd). The 6-31G** leads to results that represent a compromise between accuracy and computational cost, and for simplicity, only the results obtained with this basis set were included in the present manuscript. Moreover, some of the molecules studied here are relatively big, and thus they cannot be computed to higher basis set than 6-31G**. All these levels appear implemented in the GAUSSIAN 03 program package [44]. The UNIX version with standard parameters of this package was running in the alpha computer of the Complutense University of Madrid.

The optimum geometry was determined by minimizing the energy with respect to all geometrical parameters without imposing molecular symmetry constraints. The TIGHT convergence criterion was used. Calculation with Tomasi's polarized continuum model (PCM) was used as implemented in Gaussian 03 by default using the integral equation formalism model, IEF-PCM. All the molecules were optimized in the cationic form. Molecules I, II, IV, W84, DUO-3O and DUO-3C have two positive charges, while the remaining molecules have only one positive charge. Atomic charges were determined with the Natural NBO procedure [45, 46].

For each compound under consideration, calculations of harmonic wavenumbers were carried out to assess the true minimum forms. It was performed at the same level of the respective optimization process and by the analytic evaluation of the second derivative of the energy with respect to the nuclear displacement. All the optimized structures showed positive harmonic vibrations only (true energy minimum). Relative energies were obtained by including zero-point vibrational energies (ZPE). For the calculation of the ZPE, the wavenumbers were retainted unscaled.

Results and discussion

General characteristics of the allosteric modulators

A common feature of the different structures of AM's is the existence of two or three positively charged nitrogens. These atoms appear to play an important role in the attachment to the receptor [5, 23, 24, 47]. The factors contributing to the stabilization of the complex structure include complementarily of shape, H-bonding, and electrostatic and hydrophobic properties. Conformational (superposition) studies of bisammonium (hexamethonium-type) and bispyridinium (DUO-series) compounds have reported that the main factors affecting the conformation are both: the mutual electrostatic repulsion between the two charged moieties, and the π–π interaction between the two aromatic rings [16]. Thus, two geometrical parameters can be of interest: (1) the distance between the mass centres of the terminal aromatic rings, and (2) the distance between the two formally charged nitrogens [16]. This latter distance, $d(N^+\cdots N^+)$, has shown to be relevant for activity, and its optimal value has been reported [23, 24] to be about 9.7 Å, Table 1.

A previous investigation revealed[48] that in AM's only one half of the symmetrical shape is important for the

Table 1 Calculated values of the $N^+\cdots N^+$ and $N^+\cdots N$ intramolecular distances in Å

Compound	$d(N^+\cdot\cdot N^+)$	$d(N^+\cdot\cdot N)$	Compound	$d(N^+\cdot\cdot N^+)$	$d(N^+\cdot\cdot N)$
IV	9.435	-	W-84 linear	9.063, 8.89[a]	5.058
Ia	9.216	5.002	the most stable	9.045	4.187
+ 15 H_2O	9.255	5.080	+ 10 H_2O	9.014	4.692
Ib	9.234	4.997	sandwich	9.067, 9.09[a]	5.031
IIa	9.253	5.052	distorted sandwich	8.641, 8.87[a]	4.810
IIb	9.285	4.980	+ 10 H_2O	8.511	4.759
			DUO-3O	9.497[b]	4.969
			+ 10 H_2O	9.406[b]	4.981
			DUO-3C	9.546[b]	4.991
			Alcuronium	9.71[a]	

[a] References [23, 24]

[b] $d\left(N^+_{\text{moiety I}}\cdots N^+_{\text{moiety II}}\right)$

allosteric action. Thus, it is reasonable to focus also on the distance between the centre of the positive charge and the nitrogen atom of the urea or carbamate substituent, $d(N^+\cdots N)$, Table 1.

Bispyridinium compounds

All the pyridine-like systems are aromatic molecules classified as π deficient compounds [49] since the pnicogen atom (in this case nitrogen) plays the role of a very electronegative center compared with carbon [47]. The bispyridinium compounds under study have certain structural features that are common in many anthicholinergic and cholinergic agents, synthesized and evaluated pharmacologically [50]. These kinds of compounds have two essential constituent groups: cationic head (mainly a substituted ammonium group) and a heavy moiety (carbamate, cyclic radicals…). A middle chain of limited length connects both groups.

The cationic head can be attached to the negative anionic center of the muscarinic receptor. This cationic head has been reported to provide the electrostatic forces necessary to start its adsorption process to the receptor. Following, weak dipole–dipole, hydrophobic and Van der Waals forces can contribute to the stability of the drug–receptor complex [50].

The middle chain of the bispyridinium-type modulators does not appear to be critical. Mainly it serves as a dicationic spacer linking pharmacophoric aromatic substituents [51].

The geometry structure of bispyridinium compounds has not been studied by ab initio or DFT methods combined with high basis set. Thus, our interest in a detailed description of our compounds under study, with comparisons with the data reported [52] by B3LYP/6-311++G** on the simple molecule of pyridine-substituted α-diketone.

Geometry optimization of our compounds in the isolated state

General considerations The different conformers are defined through τ_1 to τ'_3 torsional angles (Scheme 5) of the pyridine ring and the neighboring substituent. All structures possess C_2 rotation axis through the middle of the bond between the two urea groups, which implies symmetry-equivalence of the two pyridine-urea fragments. Scheme 5 also shows a general labeling of the atoms in the pyridinium compounds under study. The C10–C16 bond length changes depending on the attachment substituent on C10 and C16: with –H (molecule IV, Scheme 6) is 1.534 Å, with = O (pyridine-substituted α-diketone molecule) is 1.54 Å[52], with -urea (molecules Ia and Ib) is 1.547 Å, and with–ethylcarbamate (molecules IIa and IIb)

Scheme 5 Labeling of the atoms in **Ia**

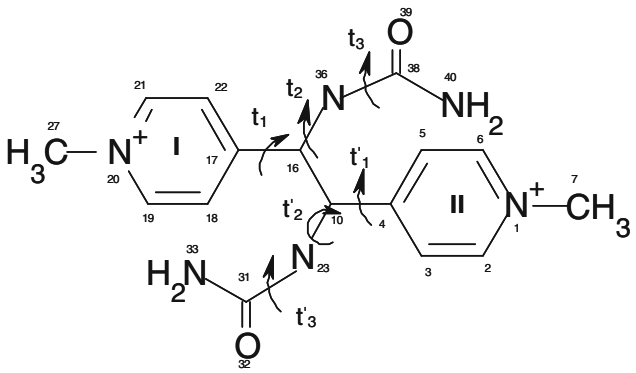

is 1.551 Å. Long values of C10–C16, as well as of C4–C10 (C16–C17) bonds, indicate a high molecular flexibility. Molecule IV is not active, while IIa and IIb with longer values than Ia are more active than Ia. The C10–C16–C17 angle also changes slightly depending on the substituent, with –H is 116.1 °, with =O is 119.5 ° [52], with–urea and with–ethylcarbamate is ca. 114.9 °.

The C4–C10–C16–C17 torsional angle between both rings remarkably changes with the substituent. With –H it is 179.86 ° (planar form), with =O is 126 ° [52], with–urea is 150.4–150.8 °, and with–ethylcarbamate is 151.9–153.0 °. Minimal substituent–substituent repulsion corresponds to a value of this angle of 180 °, value obtained in our case only with –H substituent. The maximal substituent–substituent repulsion corresponds to =O substituent. The balance between the high electrostatic repulsion oxygen–oxygen of the carbonyl group from one hand, and the conjugated oxygen–aromatic ring from another hand gives the value of this angle.

The N23–C10–C16–N36 torsional angle is the most affected parameter with the change of the substituent: 63.5 ° (with –H), 120 ° [52] (with =O), 45.2–45.4 ° (with—urea), and 45.4–46.0 ° (with –ethylcarbamate). The τ'_1 torsional angle also changes with the substituent: 56.9 ° with –H, ca. 0 ° with =O (due to conjugation with the ring), ca. 63 ° with –urea, and 62.5–61.8 ° with –ethylcarbamate.

As expected the dipole moment (μ) of IV is null. With two urea substituents (molecule **Ia**) the value slightly increases up to 0.88 D (in the most stable conformer). A remarkable increase is obtained with the lengthening of the aliphatic chain bonded to N^+ (N1 or N20), such as in molecule **Ib** (5.95 D), as well as, the substitution of the two amino groups by a O–CH_2–CH_3 moiety, such as in IIa (6.05 D).

When the negative charge on N^+ is reduced, the C2–C3 bond of the pyridine ring is lengthened as well as N^+–C7, while N1–C2 bond is shortened. I.e., the aromaticity of the pyridine ring is reduced.

Specific analysis of the different molecules (Scheme 2) *Molecule III*: it was selected to observe the influence of the methyl group on N1 in the pyridine ring structure. The molecule is planar and in the minimum the methyl groups appear in the *staggered* form, with all their hydrogens out-of-ring plane. These methyl groups produce a small deformation from the planar form in the angles involving N1 and C4. The deformation angle (*tilt* angle ε) [53] is smaller on C4 (1.0 °) than on N1 (2.0 °). In the saddle form the values are very small, 0.5 ° on C4 and 0.7 ° on N1. The slightly longer C3–C4 (C4–C5) and N1–C2 (N1–C6) bonds than on pyridine molecule [54], lead to a closening of the *ipso* angles of ca. 3 °.

In pyridine the nitrogen atom has a high negative charge, consequence of its electron lone pair, which can bond to other molecules. It produces, by electron attraction, a deficiency of negative charge in the C2 and C6 neighbour ring atoms, and an enhancement of the negative charge on the C3, C4 and C5 atoms. In molecule III, the substitution with a methyl group produces [54] a noticeable decrease, ca. 0.18 e^- in the negative charge on N1, as well as on C4 (now is positive), while the remaining atoms are not affected. Thus, the negative charge on C10 methyl carbon is much higher than on C7, and molecule III is less reactive than pyridine.

Scheme 6 Conformers **a** y **b** of molecule **IV** with the labeling of the atoms

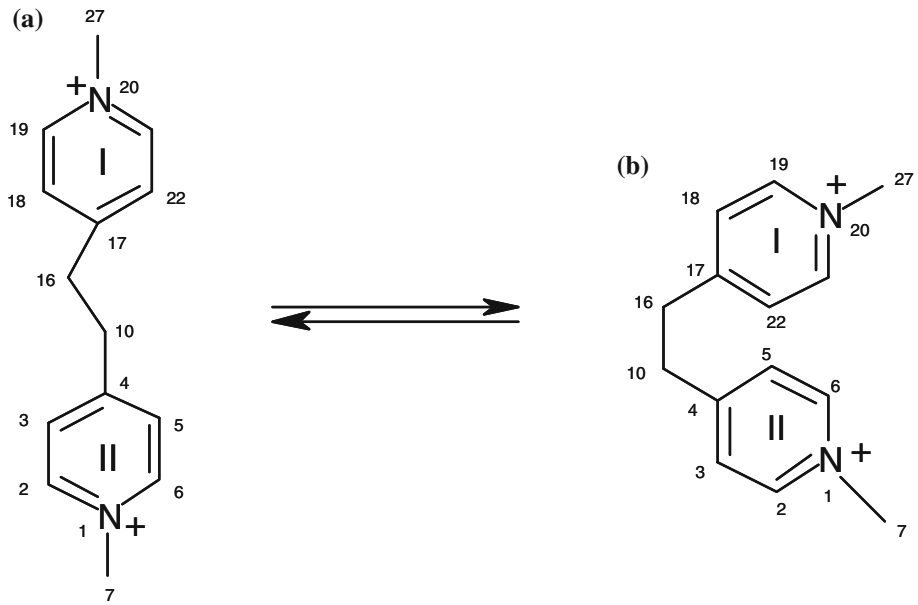

4-Alkyl substituted pyridinium salts are stable since there is a noticeable delocalisation of the electrons on the ring atoms. They posses a positive quaternary nitrogen existing in a planar arrangement (=N^+), so ligands would be able to bind at the receptor. Furthermore, substituents on the pyridine ring with a negative inductive effect reduce electron donation to the ring and thus they increase the positive charge on the nitrogen [55].

Molecule IV (Fig. 1). Although we have not synthesized this molecule, it was calculated theoretically as building block for our bispyridinium compounds. It is symmetric through the C10–C16 bond, and it shows a form **a** ↔ form **b** shift, Scheme 6, analogously to 4-styrylpyridine [56]. Form **a** was found to be planar, while form **b** is markedly twisted. The non-planarity of form **b** can be ascribed to the steric hindrance between the neighboring *ortho* H substituents of the two cyclic rings. Therefore, form **b** is less stable than form **a**, ca. 4.4 kcal/mol.

The form **a** → form **b** shift gives rise to an increase of about 3 ° in the angle C4–C10–C16 (C10–C16–C17), and it is also accompanied by a small lengthening (of about 0.004 Å) in the C10–C16 bond. The C4–C10 (C16–C17)

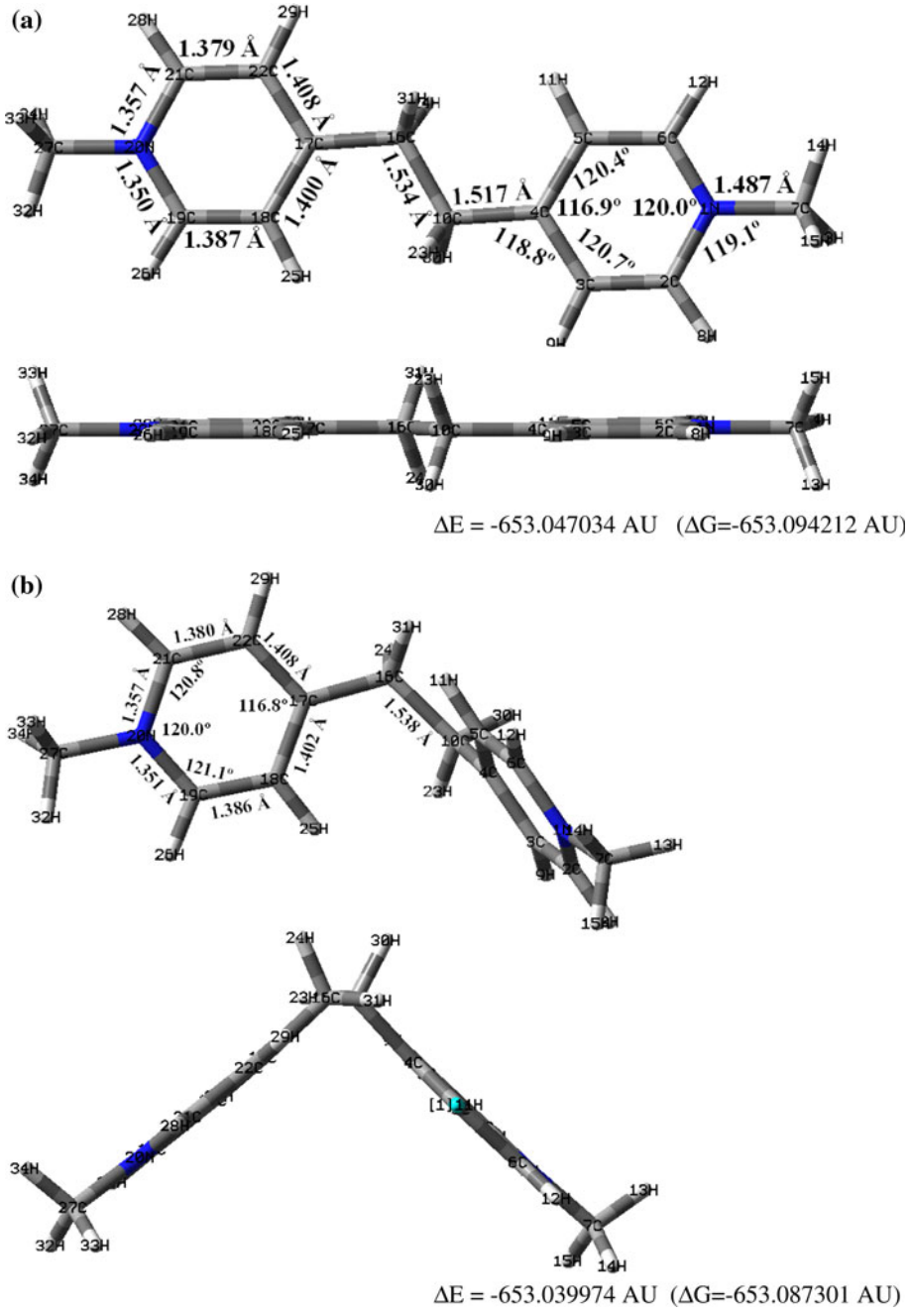

Fig. 1 Two different views of conformers **a** and **b** in molecule **IV** with values of several selected optimised geometrical parameters. The values of the electronic +ZPE energies (ΔE) and electronic + thermal free energies (ΔG) are also included

bond remains almost unchanged, 1.516 Å, in contrast to the lengthening observed in 4-styrylpyridine [56]. The non-planarity of the structure in form **b** prevents the delocalization of the π system over the whole molecule. The delocalization is therefore confined to the pyridine ring. The quinonoid character of the pyridine ring is slightly decreased as compared to molecule III.

The *tilt* angle decreases on N1 (1.2 °), but it increases significantly on C4 (3.0 °). The negative charge on N^+ is decreased, ca. 0.004 e^-, as compared to molecule III. Thus, its effect is lower on the adjacent atoms, the polarization on the adjacent C–H bonds is very small, and all the hydrogens on the ring have almost the same positive charge.

Molecule Ia. By rotation of the torsional angles τ_1, τ_2 and τ_3, and their analogous τ'_1, τ'_2 and τ'_3 (Scheme 5), seven main conformers were calculated, Fig. 2. In the bottom of each conformer, the value of the electronic +ZPE correction energies (ΔE) and +thermal free energies (ΔG) appear indicated. The most stable conformers appear when τ_3 and τ'_3 are close to 170 °. The global minimum corresponding to conformer 1 is shown in bold type. In this conformer, the two rings appear in almost the same plane (slightly tilted) as in form **a** of molecule IV, Fig. 1, while the urea substituents are placed perpendicular on this plane and symmetrically through the C10–C16 bond. Both substituents are oriented in opposite side of each other to avoid their repulsion. Thus, the urea substituent bonded to C10 appears oriented to ring I, while that bonded to C16 is oriented to ring II. Both substituents also produce a significant increase of the *tilt* angle on N1 (1.7 °) and on C4 (4.2 °), as compared to molecule IV.

Conformer 1 appears stabilized by two strong and two weak intramolecular H-bonds with a C10–H···O32 (C16–H···O39) angle of 109.3 ° (weak) and a C18–H···O32 (C5–H···O3) angle of 163.6 ° (strong). Although several methods have been suggested for the identification of the H-bonds [57], because of the size of the system, in the present work the criterion according to Desiraju et al. [58, 59]. was followed. In conformer 1 two saddle forms were determined, corresponding to a rotated $C27H_3$ group, with values of the C19–N20–C27–H torsional angle of −63.6 ° and −121.3 ° (−39.96 ° in the true minimum). In these saddle forms the value of τ_1 remains almost unchanged.

Conformer 2 is not symmetric with a difference of ca. 40 ° between τ_1 and τ'_1, ca. 30 ° between τ_2 and τ'_2, and ca. 10 ° between τ_3 and τ'_3. Only one weak H-bond through O39 stabilizes this structure, as well as in conformers 3 and 5. By contrast, in conformers 4 and 7 the stabilization is by a H-bond between the urea substituents. Finally, in conformer 6 is not observed H-bonds.

Figure 2 collects several interatomic distances of relevance. The interest of these data is their relation with the possible acceptor sites in the receptor. Electrostatic interactions have been found to be primarily responsible for molecular recognition between the allosteric binding site and the ligands. In this recognition [25] both positive charges seem to be as important as the terminal aromatic rings. Thus, the $N^+\cdots N^+$ distance has been reported [23, 24] as the most important parameter, and for activity its value should be around 10 Å. For this purpose, Table 1 collects the calculated values of the $N^+\cdots N^+$ and $N^+\cdots N$ distances in our synthesized molecules as well as in the most potent AM: the highly flexible W84 and the rigid alcuronium. For comparison purposes, the calculated values reported at a low level of theory using MM are included in Table 1. Our results are remarkably much better than the previous ones reported.

The =O···O= distance was also included in Fig. 2 because it is between the most reactive atoms. Its range of values is large 4.07–6.92 Å, due to the great flexibility of the structure. However, it is very close: 6.54–6.64 Å in the global minimum of compounds I and II.

The main effect of the urea substitution on C10 and C16 is a strongly withdrawing of the negative charge on these atoms, as compared to molecule IV. The effect on the rest of the molecule is not significant. The delocalisation of the positive charge on the pyridine ring is very close to that of molecule III, with a difference lower than 0.01 e. The differences are also low in the charge on N^+. Both pyridine structures are similar. The reactivity of the molecule is mainly through the carbonyl oxygen and the amino hydrogens of the urea group that have the highest charges.

Molecule Ib. On this molecule was carried out a similar conformational study that in Ia. The substitution of the two methyl groups by two butyl groups has not influence in the global minimum, Fig. 3, which has almost the same torsional angles that in molecule Ia.

Molecule IIa. Analogously, the substitution of the two amino groups by two $O–CH_2–CH_3$ groups has little influence in the torsional angles τ_1 to τ'_3 of the global minimum. The result is shown in Fig. 4. The coplanarity of both rings remains similar to Ia. The new oxygen atoms produce a small weakening in the intramolecular H-bonds, although it doesn't affect to the stabilization of the structure.

Molecule IIb. The substitution of the two methyl groups by two hexyl groups has not influence in the global minimum, Fig. 4, which is the same that in molecule IIa. The increase of the aliphatic chain length has little influence in the structure of the rings and in the carbamate substituent, but it produces a remarkable increment in the lipophility of the molecule.

The H-bonds appear slightly weakened as compared to IIa, although the charge on O32 is very close to IIa. I.e., its reactivity is similar. The ethylcarbamate group in IIa and IIb has a slight effect in the charges on the nitrogen atoms (N23, N36). These atoms of the carbamate moiety

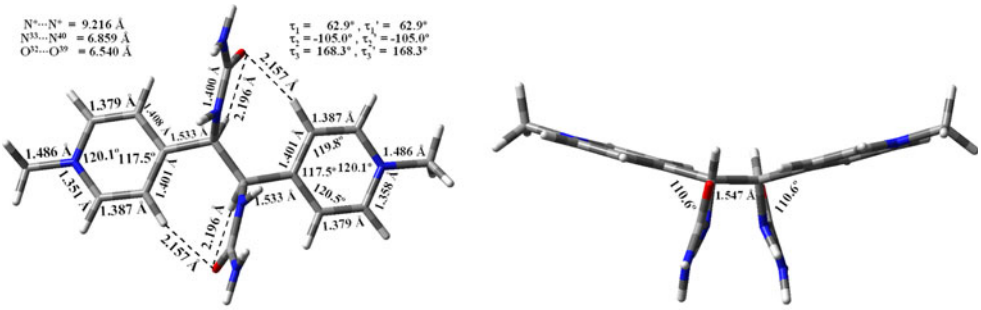

conformer 1.: ΔE=-1101.10591 AU (ΔG=-1101.16181 AU)

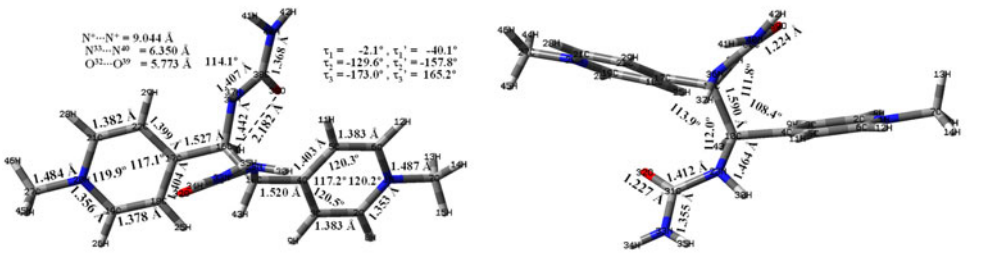

conformer 2.: -1101.098853 (-1101.155629)

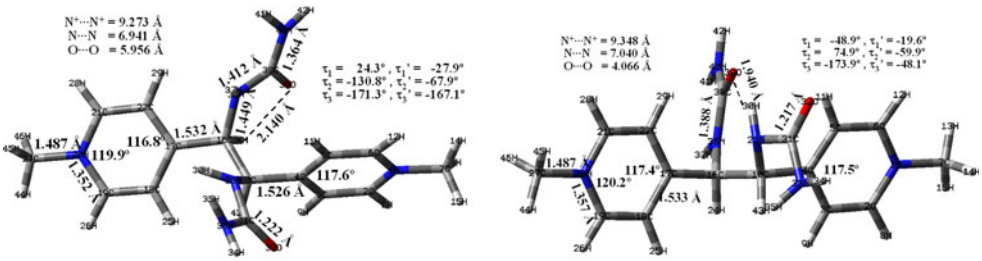

conf. 3. -1101.095976 (-1101.152999)

conf. 4. -1101.089521 (-1101.146753)

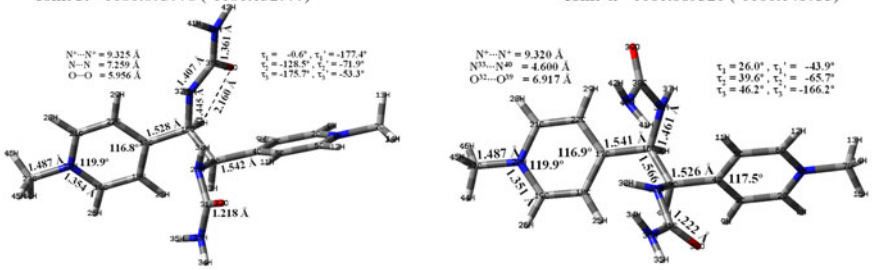

conf. 5. -1101.084684 (-1101.142305)

conf. 6. -1101.077460 (-1101.134203)

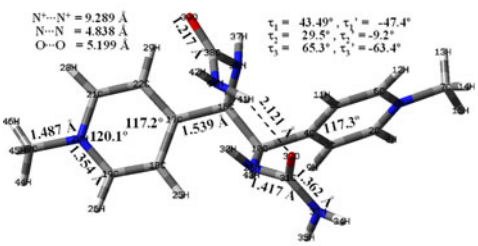

conf. 7. -1101.064911 (-1101.120015)

Fig. 2 Stable conformers optimized in molecule **Ia** with the labeling of their atoms and with the values of the most important geometrical parameters calculated at the B3LYP/6-31G** level. The most stable one, conformer 1, and the second one, conformer 2, appear plotted in two different views

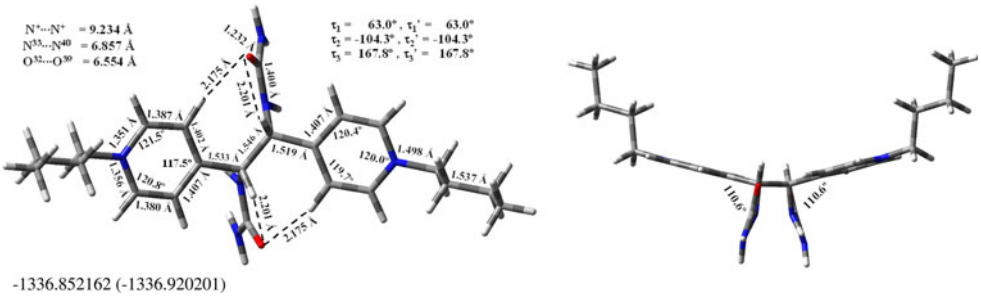

Fig. 3 Two different views of the most stable conformation optimized in molecule **Ib** with several selected geometrical parameters

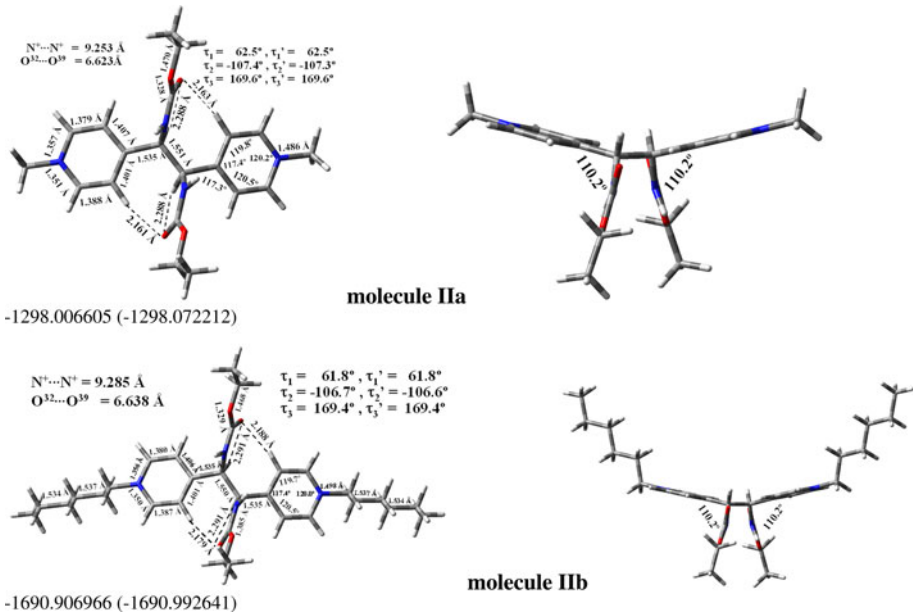

Fig. 4 Two different views of the most stable conformation optimized in molecules **IIa** and **IIb** with with several selected geometrical parameters

withdraws negative charge on the C10 and C16 bonded atoms, and leads to a slight reduction of the positive charge on C4 and C17, as compared to molecule Ia. The charges on the other nitrogen and carbon atoms remain almost unchanged. I.e., the reactivity of these molecules is similar, as we have observed experimentally.

Molecules A–D. For comparison purposes, a conformational analysis was also carried out on simpler compounds, Scheme 3. In the optimum conformation, the atomic charges on the N^+ and =O atoms (Table 2) as well as several distances of interest were analysed.

W84, DUO-3O and DUO-3C, Scheme 2b. These molecules appear today among the most potents AM's. However, they have been little studied structurally, and never by ab initio or DFT methods. For this reason, a full conformational analysis on these molecules was carried out [54]. In W84 only three conformers have been reported of interest: linear, sandwich and distorted sandwich, Table 1.

Table 2 Calculated values of the averaged atomic charge in the N^+ and =O atoms of interest

Compound	N^+	=O	Compound	N^+	=O
III	-0.306	-	W-84 linear	-0.288	-0.578
IV	-0.296	-	the most stable	-0.289	-0.614
Ia	-0.298	-0.675	+ 10 H_2O	-0.392	-0.622
+ 15 H_2O	-0.303	-0.744	sandwich	-0.289	-0.567
Ib	-0.293	-0.675	distorted sandwich	-0.292	-0.620
IIa	-0.297	-0.670	+ 10 H_2O	-0.286	-0.623
IIb	-0.292	-0.670			
A	-0.307	-0.648	DUO-3O	-0.327	-0.278
B	-0.303	-0.635	+ 10 H_2O	-0.327	-0.327
C	-0.308	-0.650	DUO-3C	-0.318	-
D	-0.307	-0.650			

The notation "N^+" for the piridinium nitrogen atom is normally used in the bibliography, but it is not related to its atomic charge value

In addition, we have included in the table the most stable conformer. By superposition studies, the distorted-sandwich is considered as the experimental one [23, 24]. DUO-3O and DUO-3 N have not been studied conformationally, and the only parameter reported of interest is its $N^+\cdots N^+$ distance.

Simulation of the hydration: first hydration shell

Water is the natural medium of all biological molecules, participating in different processes involving the living cell. Hydration of AM's is of fundamental importance because of the biological functions of them are dependent on their interactions with surrounding water. This interaction takes place through both hydrophilic and hydrophobic sites. The water molecule is a versatile connector that can serve as both hydrogen bond donor and acceptor, and contribute to the overall stability of the structure. Due to the high flexibility of our compounds, their conformers are strongly dependent on the hydration.

Experimental studies in methyl-substituted uracils and thymines indicated that when more than four water molecules are attached, the photophysics properties of these hydrated clusters rapidly approach to those in the condensed phase [60]. Thus, with our simulation of the first hydration shell with 15 water molecules, all the physical properties in solution can be clearly described.

To theoretically simulate the hydration effects three procedures have been suggested [61]. The most accurate ones is the Discrete Model (DM) by including sufficient numbers of explicit water molecules [62]. Thus, it was the main model followed in the present paper. The methodology used in the hydration was previously reported in accurate investigations on nucleosides and related molecules [63, 64].

More than 200 cluster structures with water were analyzed. The hydration reduces the number of conformers calculated in the isolated state. For simplicity, only the resulting cluster combination with 15 water molecules in conformer 1 of Ia is shown in Fig. 5. The further addition of water molecules increases the complexity of the hydration pattern, which is derived from an extraordinary variety of orientations and H-bonds displayed by the water molecules, but it does not produce significant interaction with molecule Ia, neither changes in their parameters. The main features observed in the hydration of Ia are as follows:

(i) In the most stable monohydrated form, the water molecule appears H-bonded to H23 (N23) and H36 (N36), Scheme 5, which produces a noticeable change in the angles involved in both urea substituents. This position of the water molecule remains with the successive hydration, and with 15 water molecules, Fig. 5, it corresponds to W_1.

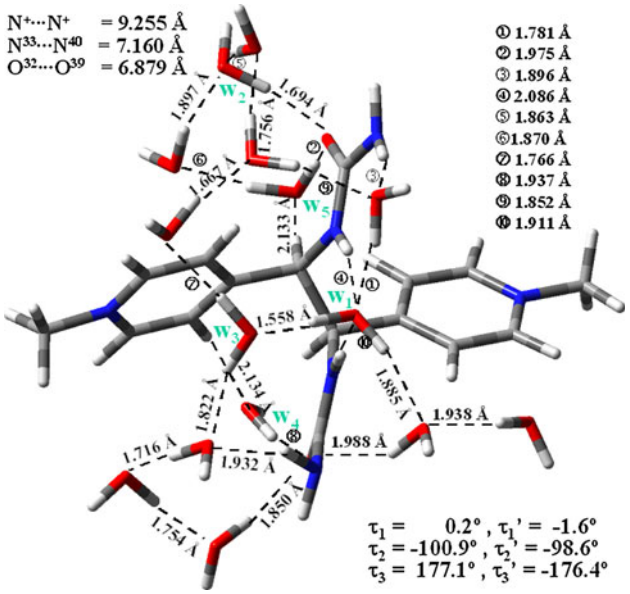

Fig. 5 View of the first hydration shell in molecule **Ia** with 15 water molecules

(ii) Due to H-bonds water-water are more stable than water-Ia, the direction of the successive hydration is marked for this first water molecule W_1. With more than six water molecules, the strength and number of H-bonds water-Ia are reduced, while H-bonds water–water are increased. In the different clusters, the optimum distribution of the water molecules binding to the most polar groups is in accordance with those found in related molecules.

(iii) The hydration produces a small lengthening (0.01 Å) of the N–H and C=O bonds involved in the intermolecular H-bonds, and by contrast, the neighboring N–C bonds shrank by 0.005 Å. As expected, the C–H bonds are not sensitive to water.

(iv) Due to the small interactions of the water molecules with the pyridine ring, the hydration little affects its planarity, less than 0.5 °. A small lengthening (ca. 0.002 Å) and closening (ca. 0.5 °) of the *ipso* ring angles involving in H-bonds are observed, as well as a small shortening of N^+–C7 (0.006 Å) and opening of C–N^+–C (0.3 °) angle.

(v) The distribution of all the water molecules along the urea substituents indicates that these substituents act as hydrophilic region, while the pyridine rings correspond to the hydrophobic region. Due to this distribution, a remarkable change is observed in the τ_1 and τ_1' torsional angles, as well as in N23–C10–C16–N36 between both urea substituents (70.6 ° vs 45.2 ° in the isolated state). The changes in the other torsional angles are small: in τ_2 and τ_2' ca. 5 °, and in

τ_3 and τ_3' ca. 10 °. The hydration shows the high flexibility in the orientation of both urea substituents.

(vi) In conformer 1 (Fig. 2) the symmetry of the molecule disappears with the hydration, and in the most stable cluster with 15 water molecules (Fig. 5) the pyridine rings are almost perpendicular. Thus, the C4–C10–C16–C17 torsional angle between the pyridine rings changes remarkably (175.9 ° vs. 150.4 ° of the isolated state), as well as C3–C4–C10–C16 and C10–C16–C17–C22 (126.3 ° vs. 168.8 °).

(vii) The water molecules appear stronger H-bonded to the oxygen atoms than to the amino hydrogens. Also, the oxygen atoms are involved in H-bonds with two water molecules, while the amino hydrogens only with one. The H-bonds with water lead to a general enhancement of the charges, especially on the oxygen atoms (Table 2), and therefore, to an increase of the reactivity. E.g., the oxygen and nitrogen atoms show more negative charge (by 0.04 e^- and 0.06 e^-, respectively), whereas the amino hydrogens are more positive, by 0.08 e^-.

(viii) W_1 is the water molecule most H-bonded to other water molecules. Its three atoms participate in strong H-bonds, one of them ($H_{w1}\cdots O_{w3}$) with the short value of 1.558 Å. W_2 is the water molecule that remains most strongly H-bonded to Ia (1.694 Å). This strength produces a weakening of the intramolecular H-bonds with the hydration.

(ix) The cluster obtained in the hydration of conformer 1 (Fig. 5) shows a higher stability than in the hydration of the other conformers. Moreover, conformer 1 appears as the most stable by the PCM model. Thus, presumably, this cluster has a higher probability of interact with the receptor. Of course, a bispyridinium like molecule (with at least 6 conformational angles) can change this optimum conformation, in order to adapt its shape to the interaction site of a receptor. But, if the orientation of the molecule in the cluster is inadequate, it could reduce the interaction or no interact. Thus, the importance of an adequate simulation of the hydration, and the correlation of the geometric parameters obtained with other drugs.

The simulation of the first hydration shell in the AM W84 and DUO-3O was also carried out [54] with 10 water molecules. For simplicity, only the $N^+\cdots N^+$ and $N^+\cdots N$ distances, and N^+, =O charges of these molecules appear collected in Tables 1 and 2. A decrease in the $N^+\cdots N^+$ distance is observed with the hydration.

Biological activity: isolated organ study

Important groups (carbamate and quaternary ammonium) governing cholinergic/anthycholinergic character are present in the bispyridinium salts **Ia-b**, **IIa-b**. Moreover, **Ia** and **IIa** salts have a 1-methylpyridinium group, which is ubiquitous among these agents. Thus, we studied their behaviour against acetylcholine using the isolated organ technique.

According to the method of Pöch et al. [30], the data are expressed in % by comparing the change of the compounds respect to the maximum effect achieved. The corresponding value of pA_2 or pD_2 is also obtained. All the compounds were tested in mixtures with the agonist acetylcholine, because its action is null or negligible in the used organ. The results are shown in Table 3 and Fig. 6.

Figure 6a–c indicate how the compounds **Ia**, **IIa** and **IIb** shift the concentration-effect curve of the agonist acetylcholine to the right, without affecting the maximal effect, a behavior characteristic of the competitive antagonist. Displacement is dose-dependent; the degree of the shift to the right is proportional to the antagonist concentration. Maximum effect values are below to those of control, so its action is never completely cancelled.

The results in **IIa** ($pA_2 = 6{,}91$) and **IIb** ($pA_2 = 6{,}65$) are in agreement with the fact that when the size of the alkyl groups connected to the nitrogen atom is increased, the activity is reduced or abolished. The influence of a steric factor is more evident among compounds in which the size of the substituents varies in the series of anthicholinergic and cholinergic compounds. By other hand, our pA_2 values are in accordance to earlier literature data referred to W-84 [65]. **IIa** and **IIb** compounds are more antagonist that **Ia** ($pA_2 = 6.02$).

By contrast, **Ib** produces a displacement to the left in the concentration-effect curve of the agonist acetylcholine (Fig. 6d), a characteristic behavior of a competitive agonist ($pD_2 = 6.03$). This opposite behavior of Ib cannot be explained easily, but the influence of geometry and charges is negligible.

Table 3 Calculated values of ED_{50} in M

	ED_{50}			
	Ia	Ib	IIa	IIb
Control	1.58×10^{-11}	1.44×10^{-11}	9.33×10^{-8}	5.25×10^{-12}
9.8×10^{-2} μg/ml	2.00×10^{-11}	1.35×10^{-11}	1.58×10^{-7}	1.17×10^{-11}
0.24 μg/ml	2.63×10^{-11}	8.91×10^{-12}	1.99×10^{-7}	1.34×10^{-11}
0.46 μg/ml	2.88×10^{-11}	7.94×10^{-12}	3.09×10^{-7}	2.23×10^{-11}

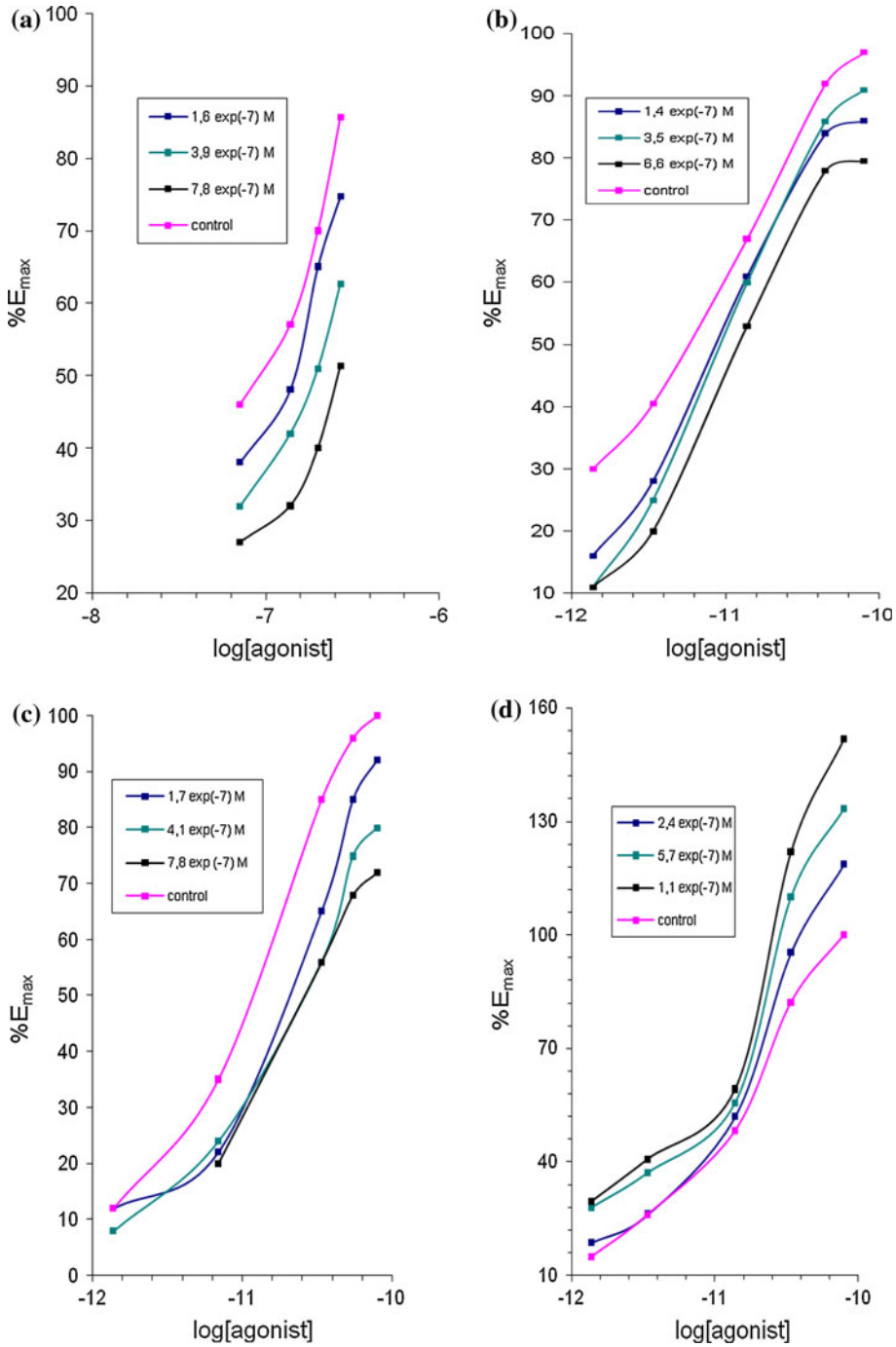

Fig. 6 Plot of response as a porcentage of maximal response versus log concentration of agonist acetylcholine. (**a**) In compound **IIa**. $pA_2 = 6.91$. (**b**) In compound **IIb**. $pA_2 = 6.65$. (**c**) In compound **Ia**. $pA_2 = 6.02$. (**d**) In compound **Ib**. $pD_2 = 6.03$

Finally, the pA_2 of simpler related compounds in *para*-substitution (Scheme 3) was determined [28], using the same experimental technique and methodology.

Relationships/tendencies observed

One of the objectives of the present work was the possibility to establish general structure–activity relationships/tendencies. Several of them are shown in Figs. 7 and 8. The relations are not totally linear, perhaps due to the value of pA_2 depends also of other parameters. Analyzing the different parameters and Figures was noted the following:

(i) A shortening of N^+–C7 (Fig. 7a) or C2–C3 (Fig. 7b) produces a decrease in the $d(N^+\cdots N)$ intramolecular distance and an increase in the pA_2 activity. The shortening in N^+–C7 and C2–C3 indicates an increment of the quinonoid character of the ring. With two exceptions, the increment in the negative charge on N23 produces an increase in pA_2 Fig. 7d.

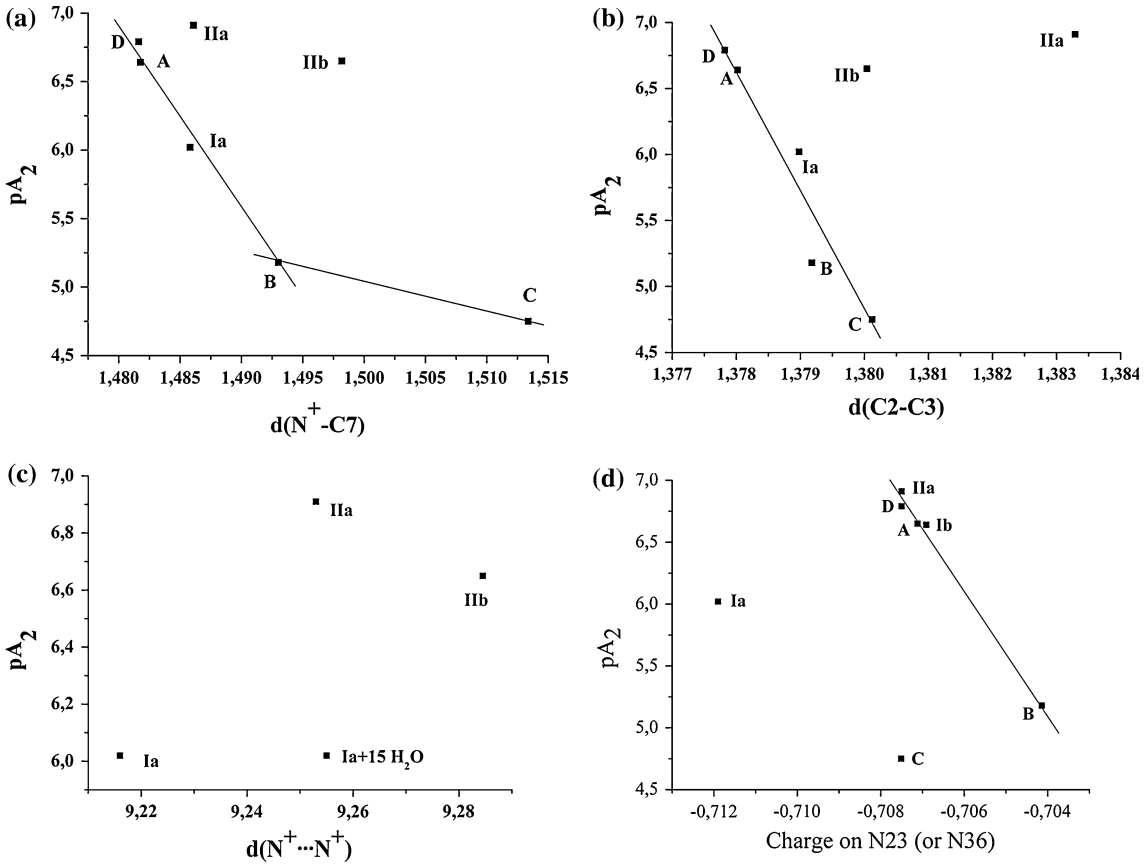

Fig. 7 Structure-activity relationships established. Bond lengths and intramolecular distances in Å

(ii) The highest activity, shortening in N^+–C7 and C2–C3, is due to an increment in the negative charge on N^+, Fig. 8a, c. This increment leads to an opening of the C–N^+–C angle (Fig. 8b) and an increase in the positive charge on C4, Fig. 8d.

(iii) Two relationships can be established in Fig. 8a depending the substituent on N^+: a methyl group (monosubstituted C7) or a chain (disubstituted C7). To confirm this feature, the calculated values in molecules III and IV, as well as in DUO-3C and DUO-3O were included in this Fig. As mentioned below, molecule C differs remarkably.

(iv) The structure of molecule C differs of the other molecules studied by its N-isopropyl group on N^+. This group produces an increase in the negative charge on N^+ (molecule C has the highest value), a remarkable lengthening in N^+–C7 (it has also the longest value), and consequently, the lengthening of C2–C3 and the lowest pA_2. Due to these features, molecule C appears in general far away in Figs. 7 and 8.

(v) Molecules IIa and IIb appear to fail in Fig. 7a, b, showing a higher pA_2 than that corresponding by their d(N^+–C7) and d(C2–C3) values. It can be due to the two pyrimidinium moieties in IIa and IIb produce a higher activity than only one: $pA_2 = 6.91$ in IIa vs 6.79 in D.

(vi) In bispiridinium compounds, the intramolecular distance d($N^+\cdots N^+$) has been considered by several authors as an important parameter related to activity. However, in our case with only three points, Fig. 7c, it cannot be demonstrated. According to the results obtained, a long distance is due to long C2–C3, C4–C10 and C10–C16 bond lengths, and a long C10–C16 indicates a high flexibility of the structure and a high activity.

(vii) In dimeric molecules (IV, Ia, Ib, IIa, IIb) the atomic charge on N^+ is lower than −0.3 e−, while in monomers (III, A, B, C, D) it is higher in negative value than −0.3 e−, Fig. 8.

(viii) In dimeric molecules an increase in the length of the substituent on N^+ produces a decrease in the negative atomic charge on N^+ (Ia –0.298 vs Ib –0.293; IIa –0.297 vs IIb –0.292).

(ix) Molecule D has one –CH_2– group more than molecule A. This additional group doesn't produce significant change in the geometrical parameters, and the slight higher activity of molecule D than

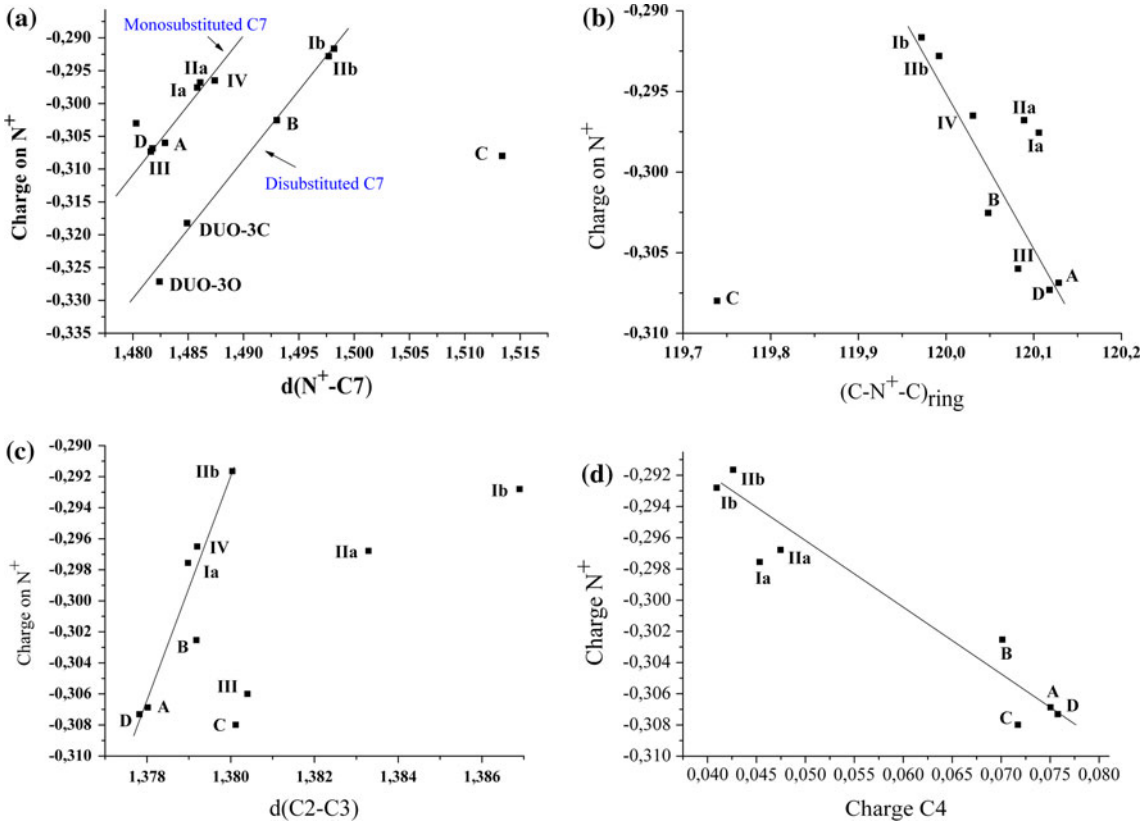

Fig. 8 Several relations established. Bond lengths and intramolecular distances in Å, and bond angles in degrees

molecule A can be attributed to a higher lipophility of molecule D than A. By contrast, the substitution of the methyl moiety by a butyl chain on C7 and the presence of a phenylcarbamate group (molecule B) produce a remarkable reduction of pA_2. In this reduction can contribute the aromatic character of the carbamate moiety.

Summary and conclusions

In the present work we have studied the molecular geometry and activity of four new potential muscarinic agents. A good agreement is obtained, whenever available, with analogous theoretical studies, supporting the quality of our results derived from computations. The most important findings of this study are the following:

(1) The different conformers of our synthesized bispyridinium salts were reproduced by B3LYP. The conformers that are symmetric appear as the most stable ones and two strong and two weak intramolecular H-bonds stabilize them. With the purpose of study their chemical reactivities, their equilibrium geometries were calculated for the first time. A similar simultaneous analysis of the potents W84 and DUO-3O allosteric modulators of the muscarinic receptor was also carried out. The geometries and values of the properties presented here appear to be the most accurate to date.

(2) For the first time, DFT methods combined with high basis set have been used to study AM's, improving remarkably the accuracy of the theoretical data reported in the bibliography.

(3) The values of the $N^+\cdots N^+$ and $N^+\cdots N$ intramolecular distances, and the values of the atomic charge in the N^+ and =O atoms of our synthesized compounds are in accordance to the values obtained in the most potent AM. These results suggest the presence in our dimers of several possible interaction points with the receptor.

(4) The positive charge is distributed on all the atoms of the molecule, slightly decreasing those with negative charge and slightly increasing those with positive charge. Small variations in the charge on N^+ lead to changes in the N^+–C7 and C2–C3 (C5–C6) bond lengths, and in the C–N^+–C angle. Many of the values appear adjusted to a linear form.

(5) For understanding its structure and possible behavior in physiological conditions, more than 200 cluster-

optimized structures with water molecules were determined at the B3LYP level. The hydration reduces the population of conformers determined in the isolated state. In the monohydration of Ia, the water molecule w_1 offers the most stable structure.

(6) The oxygen and nitrogen atoms of the urea substituents appear much more reactive than N^+ of the pyrimidine ring. Thus, in the hydration the majority of the water molecules appear H-bonded to these atoms instead of on the pyrimidine ring.

(7) The biological activity of our synthesized compounds was determined. Ia, IIa and IIb present a behavior that is characteristic of the competitive antagonist, while Ib is agonist.

(8) The highest activity is due to an increment in the negative charge on N^+, with shortening in N^+–C7 and C2–C3 bond lengths. In dimeric molecules a decrease in the length of the substituent on N^+ produces an increase in the negative atomic charge on N^+, and an increase in its activity. Long C10–C16 bond indicates a high molecular flexibility and a high activity.

(9) Our results may aid in the development of more potent and more specific agents with this interesting ability to affect muscarinic receptors.

References

1. Block GA, Martin KJ, de Francisco AL, Turner SA, Avram MM, Suranyi MG, Hercz G, Cunningham J, Abu-Alfa AK, Messa P, Coyne DW, Locatelli F, Cohen RM, Evenepoel P, Moe SN, Fournier A, Braun J, McCary LC, Zani VJ, Olson KA, Drueke TB, Goodman WG (2004) N Engl J Med 350:1516
2. Lindberg JS, Culleton B, Wong G, Borah MF, Clark RV, Shapiro WB, Roger SD, Husserl FE, Klassen PS, Guo MD, Albizem MB, Coburn JW (2005) J Am Soc Nephrol 16:800
3. Cannon JG (2003) Cholinergics. In: Abraham DJ (ed) Burger's medicinal chemistry and drug discovery, vol 6, Chap 2, 6th edn. Wiley, New Jersey, p 39
4. Krejcova G, Kassa J (2004) Acta Medica (Hradec Kralove) 47(1):13
5. Holzgrabe U, Mohr K (1998) Drug Discovery Today 3:214
6. Birdsall NJM, Farries T, Gharagozloo P, Kobayashi S, Lazareno S, Sugimoto M (1999) Mol Pharmacol 55:778
7. Ferri CP, Prince M, Brayne C, Brodaty H, Fratiglioni L, Ganguli M, Hall K, Hasegawa K, Hendrie H, Huang Y, Jorm A, Mathers C, Menezes PR, Rimmer E, Siazufra M (2005) Lancet 366:2112
8. Jaga K, Dharmani C (2005) Rev Environ Health 20(1):15
9. Ellis J (1997) Drug Dev Res 40:193
10. Birdsall NJ, Lazareno S (2005) Mini Rev Med Chem 5:523
11. Christopoulos A (2002) Nat Rev Drug Discov 1:198
12. Groβmüller M, Anthony J, Tränkle C, Holzgrabe U, Mohr K (2006) Naunyn-Schmiedeberg's Arch Pharm 372:267
13. Wess J (2005) Mol Pharmacol 68(6):1506
14. Tränkle C, Mohr K (1997) Mol Pharmacol 51:674
15. Lazareno S, Popham A, Birdsall NJM (2000) Mol Pharmacol 58:194
16. Vistoli G, Pedretti A, Villa AM, Villa L, Holzgrabe U, Cambareri A (1999) Analusis 27(1):32
17. Tucek S, Proska J (1995) Trends Pharmacol Sci 16:205
18. Soudijn W, van Wijngaarden I, Ijzerman AP (2001) Expert Opin Ther Patents 11:1889
19. Christopoulos A, Kenakin T (2002) Pharmacol Rev 54:323
20. Jakubik J, Bakakova L, El-Fakahany EE, Tucek S (1997) Mol Pharmacol 52:172
21. Dolezal V, Tucek S (1998) Br J Pharmacol 124:1213
22. Zahn K, Eckstein N, Tränkle C, Sadee W, Mohr K (2002) J Pharmacol Exp Ther 301:720
23. Holzgrabe U, Wagener M, Gasteiger J (1996) J Mol Graph 14:185
24. Nassif-Makki T, Tränkle C, Zlotos D, Bejeuhr G, Cambareri A, Pfletschinger C, Kostenis E, Mohr K, Holzgrabe U (1999) J Med Chem 42:849
25. Holzgrabe U, Hopfinger AJ (1996) J Chem Inf Comp Sci 36:1018
26. Gilsbach R, Groβmüller M, Alptüzün V, Erciyas E, Tränkle C, Holzgrabe U, Mohr K (2003) Neurochem Res 28(3/4):667
27. Braña MF, Castellano JM, Miguel PD, Posada P, Sanz CR, Migallón AS (1994) Tetrahedron 50(33):10061
28. Villarino AL (1989) Ph.D thesis. Universidad complutense, Madrid
29. Ozakca I, Arioglu E, Guner S, Altan VM, Ozcelikay AT (2007) Pharmacology 80(4):227
30. Pöch G, Brunner F, Kühberger E (1992) Br J Pharmacol 106:710
31. Seminario JM, Politzer P (eds) (1995) Modern density functional theory: a tool for chemistry, vol 2. Elsevier, Amsterdam
32. Becke AD (1992) J Chem Phys 97:9173
33. Becke AD (1993) J Chem Phys 98:5648
34. Lee C, Yang W, Parr RG (1988) Phys Rev B37:785
35. Hoffmann M, Rychlewski J (2002) Rev Modern Quantum Chem 2:1767
36. Yurenko YP, Zhurakivsky RO, Ghomi M, Samijlenko SP, Hovorum DM (2007) J Phys Chem B 111:6263
37. Yurenko YP, Zhurakivsky RO, Ghomi M, Samijlenko SP, Hovorum DM (2008) J Phys Chem B 112:1240
38. Alcolea Palafox M, Nielsen OF, Lang K, Garg P, Rastogi VK (2004) Asian Chem Letts 8:81
39. Alcolea Palafox M, Rastogi VK (2002) Spectrochim Acta 58A:411
40. Alcolea Palafox M (1998) Recent Res Devel Physical Chem, Transworld Research Network, India, 2
41. Alcolea Palafox M (2000) Int J Quantum Chem 77:661
42. Alcolea Palafox M, Iza N, Gil M (2002) J Molec Struct (Theochem) 585:69
43. Fernández-Quejo M, De la Fuente M, Navarro R (2005) J Molec Struct 744–747:749
44. Frisch MJ, Trucks GW, Schlegel HB, Scuseria GE, Robb MA, Cheeseman JR, Montgomery JA Jr, Vreven T, Kudin KN, Burant JC, Millam JM, Iyengar SS, Tomasi J, Barone V, Mennucci B, Cossi M, Scalmani G, Rega N, Petersson GA, Nakatsuji H, Hada M, Ehara M, Toyota K, Fukuda R, Hasegawa J, Ishida M, Nakajima T, Honda Y, Kitao O, Nakai H, Klene M, Li X, Knox JE, Hratchian HP, Cross JB, Adamo C, Jaramillo J, Gomperts R, Stratmann RE, Yazyev O, Austin AJ, Cammi R, Pomelli C, Ochterski JW, Ayala PY, Morokuma K, Voth GA, Salvador P, Dannenberg JJ, Zakrzewski VG, Dapprich S, Daniels AD, Strain MC, Farkas O, Malick DK, Rabuck AD, Raghavachari K, Foresman JB, Ortiz JV, Cui Q, Baboul AG, Clifford S, Cioslowski J, Stefanov BB, Liu G, Liashenko A, Piskorz P, Komaromi I, Martin RL, Fox DJ, Keith T, Al-Laham MA, Peng CY, Nanayakkara A, Challacombe M, Gill PMW, Johnson B, Chen W, Wong MW, Gonzalez C, Pople JA (2003) Gaussian 03, Revision B.04. Gaussian, Inc., Pittsburgh, PA

45. Carpenter JE, Weinhold F (1988) J Molec Struct (Theochem) 169:41
46. Reed AE, Curtiss LA, Weinhold F (1988) Chem Rev 88:899
47. Salcedo R (2004) J Molec Struct (Theochem) 674:125
48. Botero MH, Holzgrabe U, Kostenis E, Mohr K, Tränkle C (1994) J Med Chem 37:1439
49. Garrat PJ (1986) Aromaticity. Wiley, New York
50. Sastry BVR (2003) Anticholinergic drugs. In: Abraham DJ (ed) Burger's Medicinal Chemistry and drug discovery, vol 6, 6th edn. Wiley, New Jersey, pp 109–165
51. Tränkle C, Kostenis E, Burgmer U, Mohr K (1996) JPET 279:926
52. Rogachev AY, Filatov AS, Vatsadze SZ, Zyk NV (2004) J Molec Struct (Theochem) 711:7
53. Alcolea Palafox M, Gil M, Núñez J, Rastogi VK, Mittal L, Sharma R (2005) Int J Quantum Chem 103:394
54. Material available on request
55. Whiteley CG, Ngwenya DS (1995) Biochem Biophys Res Commun 211(3):1083
56. Lawson Daku IM, Linares J, Boillot M-L (2007) ChemPhysChem 8:1402
57. Yurenko YP, Zhurakivsky RO, Samijlenko SP, Ghomi M, Hovorum DM (2007) Chem Phys Letts 447:140, and references therein
58. Desiraju GR, Steiner T (1999) The weak hydrogen bond. Oxford University Press, New York
59. Panigrahi SK, Desiraju GR (2007) J Biosci 32(4):677
60. He Y, Wu C, Kong W (2004) J Phys Chem A 108:943
61. Aamouche A, Berthier G, Cadioli B, Gallinella E, Ghomi M (1998) J Mol Struct (Theochem) 426:307
62. Williams RW, Cheh JL, Lowrey AH, Weif AF (1995) J Phys Chem 99:5299
63. Alcolea Palafox M, Iza N, de la Fuente M, Navarro R (2009) J Phys Chem B 113(8):2458
64. Alcolea Palafox M, Iza N (2010) Phys Chem Chem Phys 12:881
65. Maaβ A, Kostenis E, Mohr K (1995) Eur J Pharmacol 272:103